TIRE WET TRACTION PERFORMANCE: THE INFLUENCE OF TREAD PATTERN

A.G. Veith, B.F.Goodrich Tire Co.
R & D Center, Brecksville, Ohio 44141

The traction forces generated by a rolling pneumatic tire are influenced by a number of factors. Some important ones are: tire construction, tread pattern, tread material, vehicle speed, pavement texture and the presence of interface lubricants such as water, mud, etc. This paper is concerned with the influence of tread pattern on tire wet traction as measured primarily by the locked-wheel traction coefficient, μ_s. A first-order assessment of tire wet traction performance is obtained from ϕ, the "fractional groove volume". This is defined as the total footprint tread volume that is occupied by the tread groove void. The volume fraction is obtained from the footprint area by use of a reference groove depth of 10 mm (0.394 inch). In the 40-60 MPH range the coefficient μ_s, exponentially approaches a limiting or maximum μ_s value as ϕ is increased for straight rib (groove) tires. This maximum value is a function of external factors, mainly pavement texture and water depth. At lower speeds the exponential approach to a limiting μ_s is not found. Tires with "zig-zag" groove patterns (groove pitch and throw), show slightly inferior performance to straight rib patterns at the same ϕ values. This is attributed to an increased resistance to front-to-rear water flow through the grooves in the contact patch. This allows a larger fraction of the footprint area to be borne by a thin water film and thus promotes hydrodynamic lubrication. The influence of ϕ on 60 MPH wet cornering traction is similar to the skid behavior; an exponential approach of the cornering coefficient to a limiting value, as ϕ is increased. The influence of pavement macro-texture, characterized by its void volume, is very similar to the void volume of the tire tread pattern. Pavement texture numbers which are proportional to the void, were obtained from outflow measurements with a drainage meter. The 45 MPH locked-wheel skid coefficient of a standard tire increases in an exponential manner as pavement texture is increased and approaches a maximum value analogous to the behavior with varying tread groove void and a standard pavement. The relationship of these experimental findings to tire wet traction performance in terms of vehicle operational severity is discussed.

Introduction

Tire traction is defined as the ability of a rolling pneumatic tire to generate tangential forces in the tire-pavement contact interface. These forces are of two types; longitudinal or fore-aft and lateral and are generated by frictional coupling between tire and pavement. Their magnitude is a function of the properties and characteristics of the tire and tread, the pavement, vehicle velocity, and the environmental conditions. Tire traction is important since the control of a vehicle is dependent upon these factors.

The magnitude of traction forces developed by tires covers a broad range. Maximum values are found for dry, clean abrasive textured pavements, while minimum values are experienced when a contaminating and/or lubricating material covers the pavement eg. ice, water, mud, oil.

Despite the complexity of real-world conditions that influence traction, the major factors can be listed. See Appendix I for a definition of terms.

1. Pavement Factors (macro and micro texture, contaminants and lubricants, roadway texture and layout).
2. Tire Factors (tread material, tread pattern geometry, construction features).
3. Vehicle Operation Factors (speed, cornering and braking requirements, load transfer).

This paper is devoted to the influence of tread pattern geometry on tire traction. In discussing the influence of this factor it is necessary that other factors be duly considered. It is not possible to study any one factor in isolation.

Tire Traction in Tire Use: A First-Order Analysis

The desires of the tire manufacturer and of the tire user are essentially identical. The user desires tires with a high level of traction under all possible conditions consistent with other required tire properties. The manufacturer cannot design tires that give a constant high level of traction in all environmental or tire-in-use conditions. This is prevented by certain physical and chemical laws of nature that unfortunately cannot be repealed. These natural laws and their influence on traction constitute a large part of the subject of this paper.

Tire-Pavement Frictional Coupling

The rolling or sliding tire has an apparent area of contact that is defined by the contact patch's ground plane periphery. The portion of the apparent contact area which is actually in contact, is determined mainly by the softness of the tread rubber and by the texture (macro texture) of the pavement. In the absence of contaminants real contact is intimate and lateral (cornering) forces and braking forces can be high. When a lubricant such as water is present on the pavement the contact is a lubricated one. The lubricant decreases the frictional coupling or "grip" and decreased traction is experienced. Extensive work in the field of lubrication (1), (2), (3) shows that the tire-pavement lubricated contact can vary between two main types. The simplest is defined as boundary layer lubrication where the thickness of the water layer separating rubber and pavement is of the order of molecular dimensions. The second type of lubricated contact consists of an order of magnitude thicker film of water; this is referred to as fluid film or hydrodynamic lubrication. In boundary layer lubrication the frictional force between two contacting bodies is a function of the properties of the contacting solids and of the lubricant at their common interface.

In classical fluid film or hydrodynamic lubrication the frictional force developed is strongly dependent on the bulk properties of the lubricant, mainly the viscosity, and on the velocity gradient in this film which is several times thicker than the asperity heights of contacting surfaces. There are intermediate conditions of lubrication; a mixture of both types. This mixed lubrication regime has recently been reviewed by Dowson (2). Much of the complexity of this mixed lubrication can be explained by the phenomenon of elastohydrodynamic lubrication. In classical hydrodynamic lubrication, a lift or pressure between the sliding bodies is developed from the fluid flow when a film is trapped between non-parallel approaching surface areas. No deformation is assumed in either surface. Elastohydrodynamic lubrication may be defined as a condition in which elastic surface deformation plays a significant role in the hydrodynamic lubrication process. Figure 1 shows simplified surface asperity contact conditions for the two classical extremes; hydrodynamic (asperities separated) and boundary (asperities contacting) and the two intermediate types where surface deformation plays a role.

The wet traction behavior of tires can be explained in terms of these lubrication modes. The elastohydrodynamic mode is especially important due to the low modulus of rubber compared to the road aggregate materials. This leads to easy deformability. Several investigators have reported on hydrodynamic and associated squeeze film effects in regard to tire traction. See Moore (1). In this paper the term hydrodynamic will be used for either mode ie. elastohydrodynamic or classical hydrodynamic, however the elastic mode is almost certainly of major importance in tire traction.

Figure 1. Lubrication Modes (after Dowson).

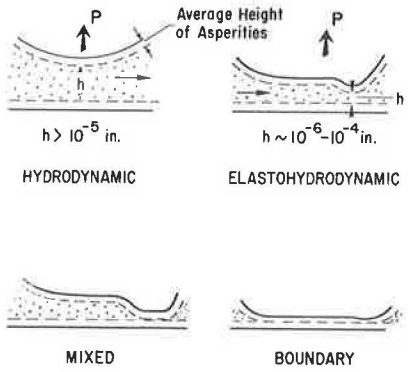

The application of hydrodynamic and squeeze film theory to tires is clarified by considering the "three zone concept". Gough (4) originally suggested this for sliding locked-wheel traction and Moore (5) carried the concept further to cover the case of a rolling tire. This concept is illustrated in Figure 2. Zone 1, the "water wedge", is formed due to the displacement inertia of the intercepted water film. In zone 2 a mixed lubrication regime exists part hydrodynamic, part boundary. In zone 3, boundary layer lubrication is dominant. The general traction vs. speed relationship of tires can be explained on the basis of the three zone concept. The zones as indicated will vary in length according to test conditions.

Figure 2. Three Zone Concept for Tire Contact (Wet).

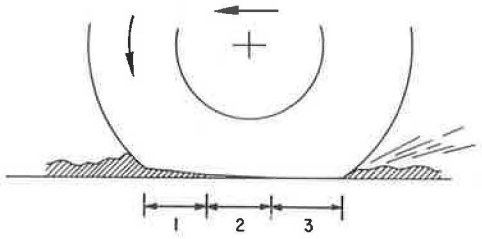

As speed increases the "water wedge" or sinkage zone, will reduce the zone 3 contact length compared to a dry pavement and the initial adhesion zone is shifted rearward. The ability to generate tangential stresses in zone 2 will be seriously reduced due to the mixed lubrication. Tire traction performance will depend upon the combined influence of the three factor groups cited above.

Conditions of High Traction Demand

The three factor groups previously listed will be considered in turn. The major characteristic of pavements is the surface texture. There are two main texture classifications, microtexture, or fine scale surface roughness in the range of 0.1 mm and below and macrotexture, which is characterized by

the average size of the visible aggregate particles and/or the intervening voids whose dimensions are one mm are greater. The properties of the aggregate influence texture and therefore skid resistance, mainly through their morphology (angularity or roundness) and their resistance to polishing due to traffic. It is generally agreed that polishing is an important characteristic of aggregates. Laboratory tests have been developed to measure this polishing tendency (6).

The influence of both types of texture on skid resistance is well documented (7), (8), (9). Low levels of both micro and macro texture and a lack of aggregate angularity contribute to a low skid resistance. More will be said in succeeding sections about the exact influence of tire factors, but it has been amply demonstrated that good wet traction performance requires an open tread pattern, one that allows adequate water drainage or discharge through the contact zone. The role of vehicle operation factors in traction is an important one. With extremely high macrotexture pavements excepted, available traction drops with an increase in speed. Vehicle operation that involves rapid accelerations, longitudinal or lateral, is also important.

The foregoing discussion has been a brief preliminary to the formulation of a concept that is required for a realistic approach to developing a tire wet traction evaluation technique. One can conceive of "operational severity" in tire use or tire testing. When operational severity is high the demand for traction is high and the traction reserve or available traction is normally low. Operational severity can be expressed in the form of a functional relationship by the following equation.

$$\text{Operational Severity} = f\left(\frac{V,\ D_W}{Tx_F,\ Tx_L, \nu_{TR},\ P_T}\right) \quad (1)$$

This equation indicates the general response of operational severity to the factors in the equation; vehicle speed (V), water depth (D_W), pavement microtexture (Tx_F), pavement macrotexture (Tx_L), void content of the tire tread pattern (ν_{TR}) and other tire factors or parameters (P_T). This concept has been discussed in a previous publication (17). Increases in V or D_W increase operational severity; increases in Tx_F, especially Tx_L and ν_{TR} decrease operational severity. For a rigorous evaluation of tire wet traction performance, the evaluation should be made under high operational severity conditions. This means high speed, deep water films and on low texture pavements. Under such critical and demanding conditions the influence of tire factors are realistically evaluated in a "worst possible case" sense.

Do such high operation severity conditions have any relationship to real-world wet accident rates? The answer is definitely yes according to a recent publication of the Highway Safety Research Institute, Univ. of Michigan (10). In summary the results of this work indicate that the combination of highway curves with certain highway grades (up or down-hill road configuration), and certain berm and superelevation conditions create high accident sites. The specific berm and superelevation conditions create deep water films at these locations due to rainfall run-off. Depths of 1 to 1.3 mm (0.04 to 0.05 inch) were reported. Williams (11) has recently reported on a survey of pavement skid resistance. Accident rates increased significantly at pavement sites with low skid resistance. Approximately 29% of the pavements measured in country-wide survey were below the accepted skid number of SN of 32. He concludes with a recommendation that a slippery surface (20-25 SN) be included in a test procedure for tire traction grading. (SN = μ_s x 100 for ASTM E-501 Tire Tested according to E-274).

Tread Pattern - Its Influence on Wet Traction

The analysis, literature review and discussion of the previous sections permit an appreciation of the influence of tread pattern on wet traction. Without this background certain aspects of tire performance are difficult to explain. Often contradictory test results are obtained. It is self-evident that some degree of tread groove void is needed for good wet traction. The question is how much void is needed and how does operational severity influence the required amount of void? This topic will now be considered.

Fractional Groove Volume

Commercial tread patterns have widely varying geometries. A simplifying and unifying variable that will represent this wide diversity for patterns is the "fractional groove volume", ϕ. "Fractional groove volume" is defined using the geometrical variables illustrated in Figure 3. It it the fraction of the total volume occupied by the grooves, referenced to the volume encompassed by (i) the developed tread width (d_{TW}) and (ii) an arbitrary reference dimension h_o, which is set equivalent to 10 mm. In Figure 3 the product $(d_{TW})h_o$ represents the reference or standard cross-sectional area of any tire. This cross-sectional area rotated through the full tire circumference is defined as the total tread volume. The total cross-sectional area of the grooves of Figure 3 is $W_G\ h_G\ N_G$, where N_G is the number of grooves. This groove area also rotated through 360° is the total groove volume. The ratio of the groove volume to the total tread volume is ϕ.

Figure 3. Tire Tread Cross-section, with Defined Dimensions.

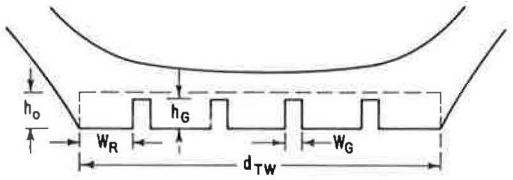

Thus

$$\phi = \frac{\text{Groove Volume}}{\text{Ref. Tread Volume}} = \frac{W_G\ h_G\ N_G\ \Pi d}{d_{TW}\ h_o\ \Pi d} \quad (2)$$

Where Πd (d=tread band diameter) indicates rotation through the tire circumference at the tread mid-point. For simple straight rib tires ϕ is given by the ratio of the two corresponding cross-sectional areas.

For more complex patterns, ϕ cannot be easily calculated from dimensions as shown in Figure 3 but must be obtained experimentally. For this purpose loaded footprints obtained with suitable inking of the tire tread may be used. From such prints the groove footprint area, the rib footprint area and the total area may be obtained. The ratio of groove area to total area is the fractional

groove area, F_{GA} and this may be used to calculate ϕ. Footprints have the advantage that static loaded groove closure is accounted for, this is more representative of actual tire use conditions.

Thus

$$\phi = \frac{F_{GA} \quad h_G}{h_o} \qquad (3)$$

Where h_G is average groove depth measured with a standard tread gage.

To evaluate the viability of the fractional groove volume concept, a series of experimental tires were prepared by hand cutting techniques. The series included both simple straight groove tires and more complex patterns representative of typical commercial tread patterns. Table 1 gives the details on the three sets of experimental tires prepared to evaluate the influence of ϕ. Figures 4 to 6 illustrate the footprints of Sets I, II, and III of these tires obtained at the 166 KPa (24 psi) rated load and at a tire pressure of 190 KPa (28 psi). The no pattern tire footprint is omitted. The ϕ values tabulated in Table 1 were obtained from these prints.

TABLE 1

Experimental Tire Sets

Set#	Tire	W_G	W_R	N_G	Remarks	ϕ
	1	- -	- -	0	No Pattern	0
	2	4*	15.*	7	Straight Rib	0.120
I	3	4	26.	4	Straight Rib	0.073
	4	8.5	15.	6	Straight Rib	0.310
	5	8.5	23.	4	Straight Rib	0.201
	6	6.	23.	5	Straight Rib	0.151
	7	4.	20.	5	P=20* T=8*	0.140
	8	4.	20.	5	P=40 T=8	0.117
II	9	9.	18.	4	P=20 T=8	0.235
	10	8.	21.	4	P=40 T=8	0.202
	11	8.2	13.5	6	Transverse Grooves	0.421
	12	8.2	13.5	6	Transverse Grooves	0.264
III	13	4.5	2.6	4	Transverse Grooves	0.144
	14	4.5	25	4	Transverse Grooves	0.126
	15	3.5	16.4	6	P=16.5* T=3*	0.159
	16	5.9	14.6	6	P=16.5 T=3.	0.257
	17	6.2	13.7	6	P=16.5 T=3.	0.266
IV	18	3.5	11.8	8	P=16.5 T=3.	0.211
	19	5.3	9.9	8	P=16.5 T=3.	0.312
	20	4.0	15.6	6	P=18.7 T=4	0.182
	21	3.8	14.4	6	P=17.7 T=5	0.188

(*measured footprint dimension (mm.) P= Pitch, T= Throw)

Figure 4. Five Straight Rib Patterns (See Table 1 for details).

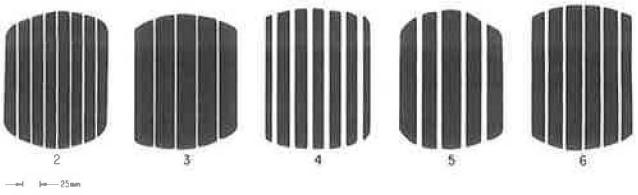

Figure 5. Four Rib Patterns with Pitch and Throw (See Appendix IV).

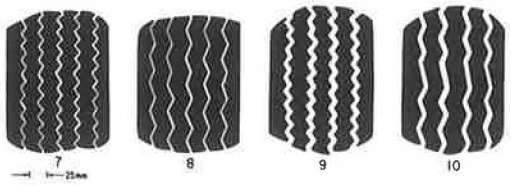

Figure 6. Four Straight Rib Patterns with Transverse Grooves in Crown Region.

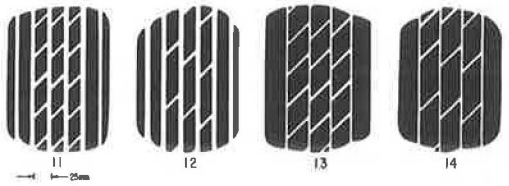

The ϕ vs Traction Relationship

To assess the influence of ϕ, measurements in two traction modes were made. Major effort was devoted to the full-skid or locked wheel wet traction coefficient, μ_s. Some data are also reported on the wet cornering coefficient, μ_c. See Appendix I for term definitions and Appendix II for test procedure details.

These two traction coefficients were selected because they both represent "quasi-static" conditions at the tire-pavement interface. Quasi-static implies that successive time averages of the coefficient should be reasonably uniform under uniform pavement - water depth conditions. In distinction to this is the peak braking coefficient which is a transient phenomenon with a varying time average sequence. Peak braking coefficient is thus more complex than μ_s or μ_c and is more likely to be influenced by external conditions and by interactions of the tire with the measuring system.

Wet traction measurements were conducted primarily on Test Surfaces G and J as outlined in Appendix II. Some data were obtained on Surface A. These are low traction surfaces that have approximate skid numbers (ASTM E-274, 64 KPH) of 16, 29 and 24 respectively for A, G and J. External water application was used and water depths averaged 1.8 and 1.4 mm respectively for G and J. See Appendix III for details on water depth measurement.

Figures 10 and 11 are plots of μ_s vs ϕ for Tire Set 1 of Table 1. Both show, for the 64 and 90 KPH (40 and 60) plots, a gradual rise in μ_s as ϕ is increased. The 32 KPH (20 MPH) plot of Figure 10 shows an initial rapid rise in μ_s which reaches a general plateau level at about $\phi = 0.08$. On both surfaces and at all speeds the distinguishing feature is the attainment of a maximum or limiting value of μ_s. The general shape suggests an exponential approach to this limiting μ_s value.

The equation,

$$\mu_s = (\mu_s)_m - K e^{-k_2\phi} \qquad (4)$$

has been found to closely represent the data where $(\mu_s)_m$ is the maximum or limiting μ_s value and the k's are constants. Rather than use the equation in the form shown in (4) it is useful to represent the rise in μ_s by a function that puts this increase on a relative basis. The advantages of doing this will become evident in the subsequent discussion.

Figure 10. Plots of μ_s vs ϕ for Tire Set I on Surface J at 32,64,96 KPH (20,40 and 60 MPH).

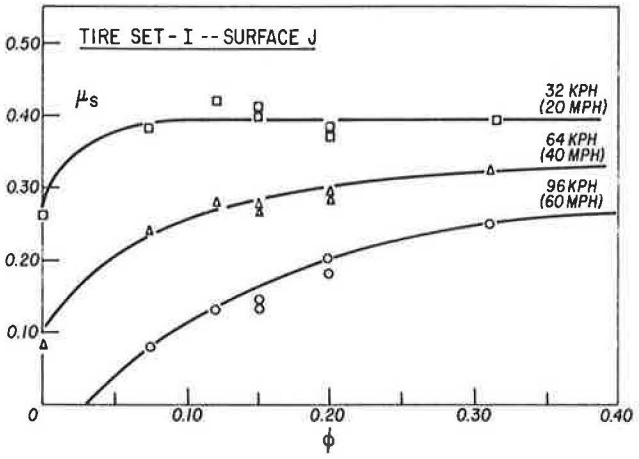

Figure 11. Plots of μ_s vs ϕ for Tire Set I on Surface G at 64 and 96 KPH (40 and 60 MPH).

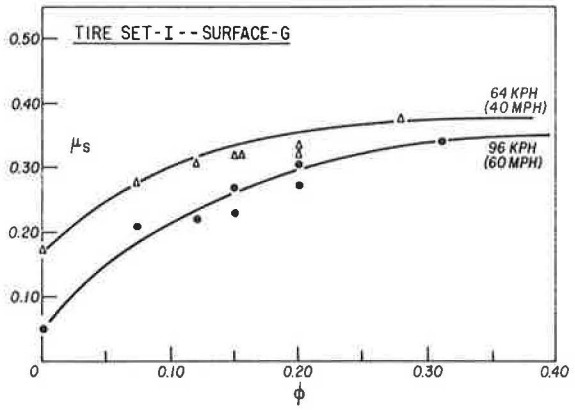

Rearranging (4) and dividing both sides by $(\mu_s)_m$, equation (5) is obtained.

$$\psi = \frac{(\mu_s)_m - \mu_s}{(\mu_s)_m} = k_1 e^{-k_2\phi} \qquad (5)$$

where $k_1 = K / (\mu_s)_m$

The quantity defined by ψ may be termed the "unused traction potential". It is evident that ψ will exponentially approach zero as ϕ is increased. Thus the value of ψ yields the potential traction yet to be realized, under any given external tire conditions, by an increased in tread void fraction, ϕ. The term $(1 - \psi)$ is the traction potential that has been used or realized, again expressed as a fraction.

Figures 12 and 13 are plots of log ψ vs ϕ which should be linear if equations (4) and (5) hold. The correlation coefficients, in the 0.90 - 0.95 range, are shown appended to the lines. The subscript, s, indicates skid or μ_s data. To prepare these plots, graphical estimates of $(\mu_s)_m$ were obtained from the curves of Figures 10 and 11. While some experimental uncertainty exists in this operation, the $(\mu_s)_m$ are sufficiently accurate to allow the log ψ vs ϕ plots to be made. The satisfactory linearity of the log ψ vs ϕ plots demonstrates the exponential character of the ψ vs ϕ relationship for the simple tread patterns of Set 1.

Figure 12. Plot of ψ_s vs ϕ for Tire Set I on Surface J at 64 and 96 KPH (40 and 60 MPH); R = Correlation Coefficient.

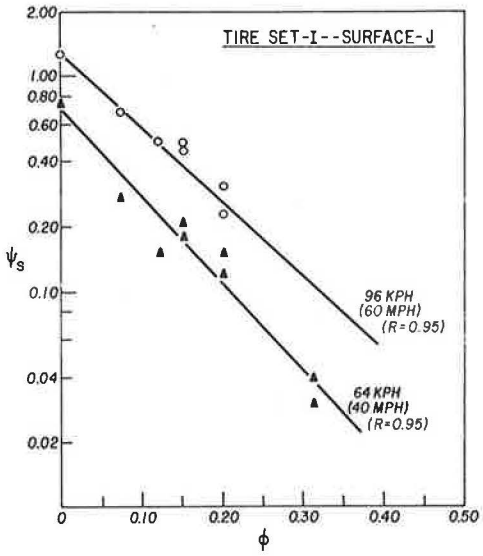

Figure 13. Plot of ψ_s vs ϕ for Tire Set I on Surface G at 64 and 96 KPH (40 and 60 MPH); R = Correlation Coefficient.

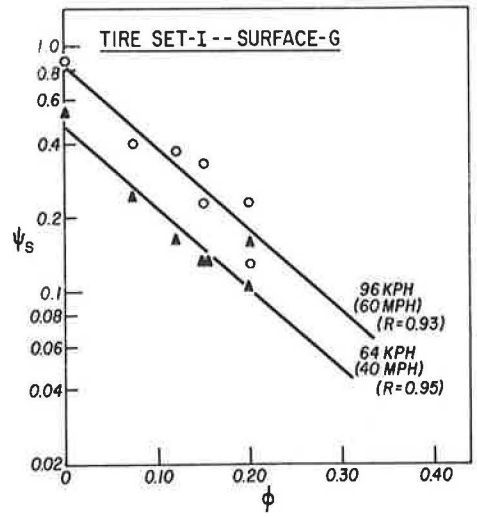

The behavior of the more complex tread patterns of Set II and III are illustrated for Surface J in Figure 14. Set II has a degree of groove "zig-zag" geometry and Set III consists of straight rib patterns with transverse grooves in the crown area. See Figure 4 - 6. The influence of groove "zig-zag" geometry is shown by the points connected by dotted lines for 32,64,96 KPH (20,40 and 60 MPH). At all speeds the presence of groove pitch and throw lowers μ_s, compared to an equal ϕ value for straight rib tires. The same situation holds for Surface G, not shown. Appendix IV and Figure 15, therein, explain the terms pitch and throw. As groove pitch is lowered the traction deficit (increased vertical displacement from the curve) is increased. See dotted arrows.

Figure 14. Comparison of Measured μ_s at various ϕ. Values in parenthesis appended to the points are the pitch values in mm. The open symbols are for Set II. The closed symbols for Set III.

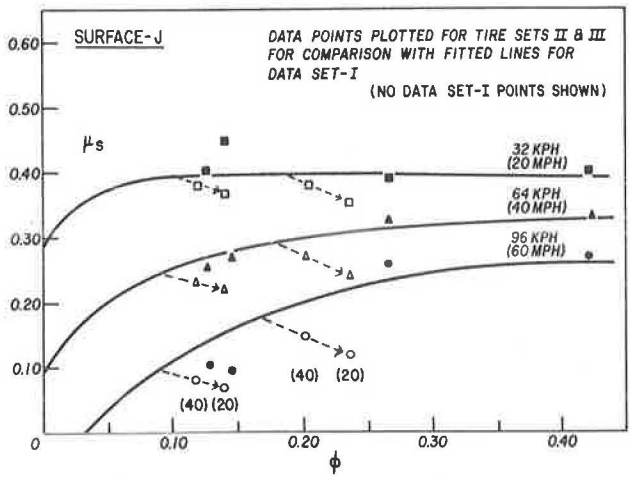

The points for Set III at the higher ϕ values are in reasonable agreement with the established straight rib curve. At lower ϕ values, the fit of Set III points is good only at 64 KPH (40 MPH) with opposite deviations at 32 KPH (20 MPH) and 96 KPH (60 MPH). These latter deviations and the pitch-throw deviations indicate that the geometric features so represented to not conform exactly to the simple exponential fit of the straight rib series. The departure of the pitch/throw points is greatest.

Figure 16. Plots of μ_s vs ϕ for Three Speeds ie. 2, 48,96 KPH (1,30 and 60 MPH) on Surface A. Closed points = nominal groove pitch, open points = larger pitch.

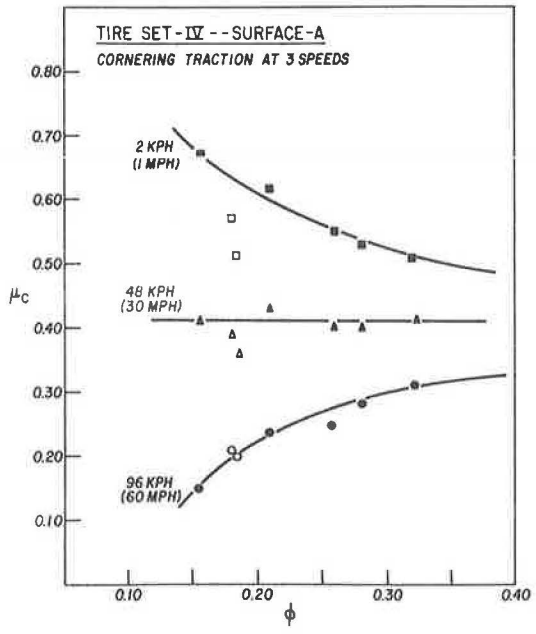

In Figure 16 plots of cornering coefficient μ_c vs ϕ are shown for Surface A at three speeds for tires designated Set IV. Widely divergent behavior is found for the three speeds. At 2 KPH (1 MPH) the approximate speed for most flat-bed tire force and moment machines, a decreasing wet μ_c is evident as ϕ increases. At 48 KPH (30 MPH) there is no significant change in μ_c over the entire range of ϕ, while at 96 KPH (60 MPH) there is an increase in μ_c that appears to be exponential.

Figure 17. Plot of ψ_c vs ϕ for 96 KPH (60 MPH) data on Surface A.

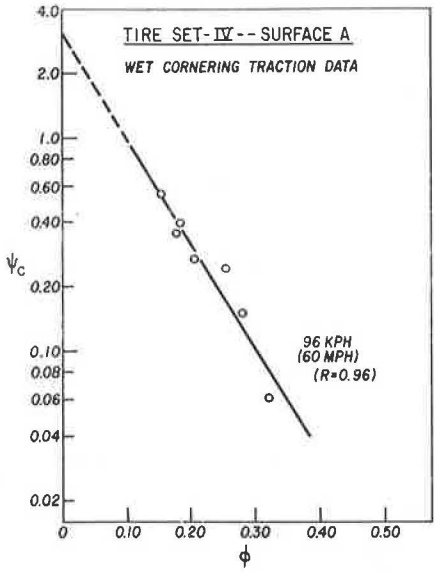

Figure 17 shows the plot of log ψ_c vs ϕ and very good linearity is found with a high correlation coefficient. Thus μ_c as well μ_s is exponentially related to ϕ.

Discussion

Footprint Phenomena

A rational explanation of the observed traction behavior is as follows. At high speeds, 100 KPH, on low texture pavements and at moderate to high water depths, the major lubrication mode is hydrodynamic. At low speeds 32 - 48 KPH (20-30 MPH) even under low texture, deep water conditions the major lubrication mode is boundary layer or mixed, with a high boundary contribution. Any measured traction coefficient is influenced by the relative proportions of these two modes. This can be expresses as:

$$\mu_{wet} = (1-F_{HL})\ \mu_{BL} \qquad (6)$$

where μ_{wet} = any measured traction coefficient

F_{HL} = fraction of footprint in hydrodynamic lubrication mode

μ_{BL} = pure boundary layer friction or traction coefficient

At very high speeds when $F_{HL} = 1$, $\mu_{wet} = 0$, and total hydroplaning occurs. Nominally this is thin-film hydroplaning as distinct from thick-film ($\sim$12mm water depth). At low speeds and especially on high

macrotexture and low water depth pavements, $F_{HL} \cong 0$, and boundary layer lubrication dominates behavior.

The plots of Figure 16 illustrate this ideally. At 2 KPH (1 MPH) increased void decreases μ_c, a well verified phenomenon for dry μ_c measurements. Since μ_c wet is lower than μ_c dry the effect of the boundary lubrication is to lower μ_c by a relatively fixed amount irrespective of ϕ. The influence of ϕ on μ_c is the same wet or dry in a relative sense.

At 48 KPH (30 MPH), F_{HL} is finite, in contrast to its zero value at 2KPH (1 MPH) and increased ϕ reduces the value of F_{HL} or enhances traction. This counter-acts the boundary layer effects evident at 2 KPH (1 MPH) and a null condition exists, no perceptible overall influence of ϕ on μ_c.

At 96 KPH (60 MPH) F_{HL} is quite high and ϕ strongly influences its value. Increased ϕ promotes efficient water drainage and reduces average squeeze paths in the footprint. The net effect of ϕ is a positive one.

The braking traction data of Figure 10 agree with these cornering data. Apart from the measured μ_s at $\phi = 0$, the remainder of the μ_s vs ϕ curve at 32 KPH (20 MPH) shows essentially no influence of ϕ on μ_c. The explanation advanced for the 48 KPH (30 MPH) cornering performance applies equally well in this case.

There is evidence in the literature to support these explanations. Schallamach (12) and Moore (5) show that the pressure sustained by thin squeeze film action is proportional to the rate of normal approach of the surfaces, this in turn being proportional to tire speed. Walters (13) reports on an analysis of the basic Reynolds thin film hydrodynamic lubrication equation. He shows that the pressure developed is directly proportional to the velocity of relative motion of sliding non-parallel surfaces. Wallace and Trollop (14) measured pressures under a rolling tire on a special test rig. They found the drag (frictional) force to be linearly related to that fraction of the total load not supported by the water film. Their results show that hydrodynamic pressure should increase linearly with speed.

The marked influence of groove pitch and throw is tentatively attributed to the combined effect of three factors. First, the increased relative channel length that groove pitch and throw contributes (See Appendix IV) is equivalent to a hydraulic resistance for groove water discharge front-to-rear in the footprint. Secondly the longitudinal braking force F_x in the contact patch has a substantial localized shear component perpendicular to the angled groove sements or walls. This causes partial groove closure and chokes off water flow front-to-rear. Third, the tires of this set have no sipes, kerfs, or slots in the rib area which during periods of impeded groove drainage, as above, can act as reservoirs or auxillary drainage paths.

It cannot be concluded that groove pitch and throw is universally detrimental. The two open points of Figure 16 plotted at each speed, represent tires with increased pitch compared to the closed points. Note that at 2 KPH (1 MPH) these points are well below the curve established by the other constant RCL points, while at 96 KPH (60 MPH) they are on the curve. Thus increased groove RCL is not detrimental for 96 KPH (60MPH) cornering traction performance in distinction to the opposite behavior for locked-wheel wet traction. Cornering traction is an important traction mode for vehicle control.

The failure of the transverse groove tires (Set III) to conform to the established straight rib curve at low ϕ is attributed to the failure of the transverse grooves to substantially contribute to front-to-rear drainage especially with narrow circumferential main grooves. The agreement of the transverse groove points with the straight groove curve at high ϕ, is due to insensitivity to changes in ϕ at large ϕ values.

Although transverse grooves do not contribute any substantial improvement in locked-wheel braking traction other than that to be expected for a given increase in ϕ (See Figure 14) they do contribute to cornering traction as Table 2 shows. An increase of ϕ from 0.21 to 0.31 due to transverse grooves yields a 43% improvement in cornering traction at 96 KPH (60MPH). The table shows that the change in ϕ associated with adding the transverse grooves yields only one-half as much improvement in the skidding traction mode as it added in cornering traction.

TABLE 2

Effect of Transverse Grooves on Traction: Wet Cornering vs Locked-Wheel

ϕ	Remarks	μ_c Relative Rating*	μ_s Relative Rating*
0.21	Rib Control Tire	100	100
0.31	Transverse Grooved Tire**	143	122

*Tested on Surface A, $D_w(aa)$ = 0.86 mm; at 96 KPH (60MPH)

**Hand cut transverse grooves 4 mm in width, 45° to circumferential line with a 50 mm circumferential spacing in each rib. (GR70x15)

The influence of small slots often called sipes or kerfs (common to many tread patterns) is illustrated in Table 3. A small positive effect is observed for the intensity of siping or kerfing as noted in the table.

TABLE 3

Effect of Shallow Sipes (Kerfs)*

		Relative Traction**	
ϕ	Remarks	32 KPH (20 MPH)	96 KPH (60 MPH)
0.180	Control	100	100
0.190	Siped Tire	105	109

*Slots cut into straight rib tires; 1 mm wide, 1.5 mm deep, 45° to circumference line, on a 10 mm spacing and open to grooves.

**Based on an average of μ_s, μ_c on Surface J and G.

The bulk of the data that indicate an exponential relationship between μ_s and ϕ were obtained from experimental hand-cut tires. Figure 18 illustrates that the exponential μ_s vs ϕ relationship applies to conventional commercial tread patterns as well. Very similar log ψ vs ϕ slopes are found and thus this exponential behavior has general applicability and is not an artifact of hand cut tires. Table 4 lists the exponential constants and correlation coefficients of the experimental and commercial tire sets. The k_2 constants for μ_s data for experimental vs commercial tires are very similar on the G and J surfaces. The tests on the experimental and commercial tire sets were not conducted at the same time

and this accounts in a large part for the differences that are found.

Figure 18. Comparison of ψ_s vs ϕ. Plots of Experimental Tire Set I vs Commercial Tires (plotted points and their fitted lines). Both on Surface G and J.

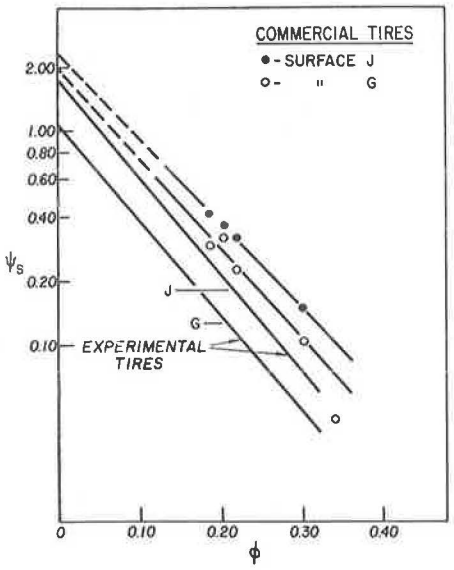

TABLE 4

Constants of Exponential Traction Equations*

Test Surface	Tire Set Tested	Type μ Meas	Speed KPH	Speed MPH	k_1	k_2	R
J	I		64	40	0.68	-9.2	0.95
			96	60	1.3	-7.4	0.97
G	I		64	40	0.46	-7.6	0.95
			96	60	0.83	-7.6	0.93
A	IV		96	60	3.3	-11.5	0.96
J	Commercial		96	60	2.2	-8.8	0.99
G	Commercial		96	60	2.0	-9.7	0.98

* $\psi = k_1 e^{-k_2 \phi}$, R = Corr. Coeff.
(AVG k_2 = -8.8)

Pavement Void vs Traction

Numerous workers (18), (19), (20), (21), have shown that a high degree of pavement macrotexture is needed for good high speed wet traction. Very often pavement macrotexture or void volume is equated with tread pattern void and it is a common observation that tread pattern void is not easily evaluated on high macrotexture pavements. One might ask whether pavement void or macrotexture influences wet traction in the same exponential manner as tread pattern void?

The answer is yes based on the data as illustrated in Figures 19 and 20. Figure 19 is a plot of μ_s vs a pavement texture number obtained from drainage or outflow measurements according to the technique of Moore (15). Details on this technique are outlined in Appendix V. Figure 19 shows an exponential increase of μ_s as N_{PT}, the texture number is increased. When the data so illustrated are treated in the same manner as described for the tread pattern data, a similar exponential behavior is found as depicted in the log ψ vs N_{PT} plot of Figure 20.

Figure 19. Plot of μ_s vs N_{PT} (pavement texture number) for Standard Straight Rib Tire at 72 KPH (45 MPH).

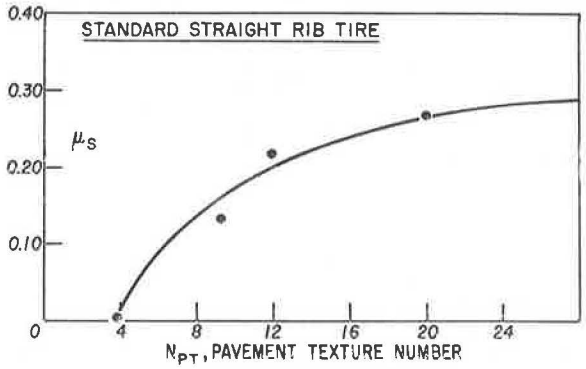

Figure 20. Plot of ψ_s vs N_{PT} at 72 KPH (45 MPH).

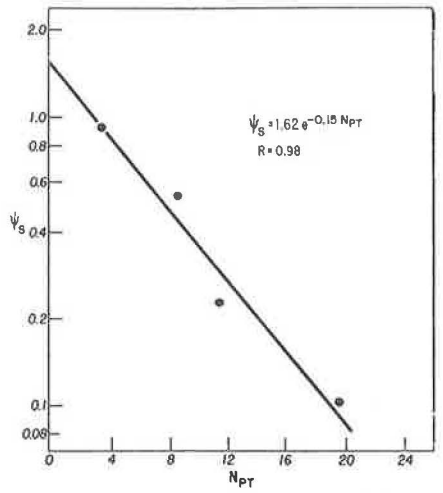

Logic argues for such exponential behavior with respect to the void of the tread as well as the void of the pavement. As the tread void is increased, under constant external tire conditions, a constant increase in traction cannot be expected. Traction must asymptotically or exponentially approach some finite limit. Similarly as pavement macrotexture or void is increased with a standard tire, speed and water application rate, traction should again approach some finite limit.

Numerous investigators (26), (27)(28) have sought a correlation of pavement macrotexture vs traction level with mixed results. Since both micro and macro-texture influence traction, a well established relationship as demonstrated in Figures 19 and 20 cannot be expected from random selection of pavements without a knowledge of both types of texture. The pavements used in this work have a very similar microtexture. Three of the four are Portland Cement Concrete and the fourth, although a bituminous - aggregate surface, has very similar aggregate microtexture as demonstrated by photo micrographs of specimens cut from the surfaces. This important fact allows the influence of macrotexture to be evaluated

free of the confusion of most highway test data where knowledge of both textures is lacking.

Tread Pattern Effect - The Literature

The influence of tread pattern on wet traction has been dealt with by a number of investigators. Albert and Walker (22) emphasized the importance of open patterns at high speeds. Simple pattern effects were evaluated and qualitative statements made about the number of ribs and grooves. They commented on the restriction of groove water drainage due to groove pitch and throw. The influence of sipes, or kerfs was studied. Most work was done on an indoor external surface smooth drum and in the cornering mode. A marked influence of sipes was found. They found that a large number of small slots was superior to a smaller number of larger slots. They postulated that the larger slots act to discharge water into the contact zone, ie. closing pressure expels the water. From on-road testing at low texture levels they found multiple knife cut slots (micro-slots) to be highly effective. Neill (23) however, found that siping (multiple 4 to 5 mm deep, cut slots) gave very small improvements in diagonal wheel stopping distance tests and J-turn cornering tests. Speeds were in the 10-50 MPH range over a variety of pavements. No preferential effect on smooth pavements was noted. Maycock (24) reported on the importance of sufficient pattern void volume at high speeds.

Kelly (25) reported on the effect of a number of tread pattern factors. He found siped tires to be superior to un-siped in braking traction only and on smooth surfaces. On pitch and throw factors there was a positive effect of throw. This was attributed to an increased wiping action. Straight rib tires however, were somewhat better under some circumstances than their pitch-throw counterparts and this was attributed to decreased resistance to flow through the groove. Performance in braking improved in going from 4 to 9 grooves but, low speed cornering showed very small effects for the same tire set.

A Return to Operational Severity

The test results set forth in this paper and in various cited references allow for a more definitive formulation of the operational severity equation.

$$\text{Operational Severity} = f\left(\frac{V^2,\ \log D_W}{T_{SF},\ (1-e^{-k_p N_{PT}}),\ (1-e^{-k_T \phi}),\ P_T}\right) \quad (7)$$

In this more realistic formulation, V^2 replaces V since stopping distance and required cornering forces vary as V^2; a logarithmic function of D_W is used, see (17); and two simplified exponential functions are introduced for pavement void or macrotexture and for tire tread pattern void. Although these changes still leave the equation in a generalized functional form, they constitute a more realistic relationship between operational severity and the parameters. Thus, speed has a very strong influence compared to D_W, N_{PT} and ϕ for example.

All commercial tread patterns can be considered as derived from basic straight rib patterns. Transverse grooves (partical or full), pitch and throw, siping or kerfing and even full block type patterns can be resolved into a basic or underlying straight rib pattern. On this basis a series of generalized μ vs ϕ curves have been constructed as shown in Fig. 21. In these plots, ϕ stands as the sole representative of tread geometry. A statistical analysis of all the μ_s data represented by Tire Sets I, II and III shows that 71% of all μ_s variation is explained by ϕ. The remaining variation (29%) is attributed to other pattern geometry features; pitch-throw and transverse grooves and to test error. Thus ϕ is the dominate component of tread pattern geometry for μ_s.

Figure 21. Generalized μ vs ϕ Relationship at Varying Test or Operational Severities.

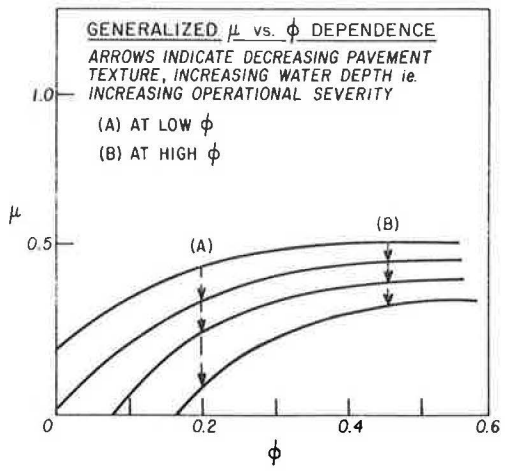

Figure 21 shows several important features inherent in the data and test results of preceeding sections but more clearly shown here.

1. Increased operational severity displaces μ - ϕ curves downward and to the right and thin-film hydroplaning may occur at finite ϕ levels at high speeds.

2. At high operational severity the influence of a change in ϕ is substantial in the lower ϕ region. Changes in ϕ are less important when ϕ is large.

3. At low operational severity the influence of ϕ is marginal over the entire range. As a result the task of evaluating differences in traction levels of tires (by μ_s) is difficult at higher ϕ levels ie. test discriminating power is lost.

4. As a corollary of 1, as ϕ is increased at any severity, the improvement in traction eventually becomes marginal and serious consideration must be given to any detrimental effect on other tire properties due to a continued ϕ increase. Thus an optimum balance exists in the design of tire tread patterns. Other important tread dependent properties are tire wear and dry pavement lateral handling characteristics.

Summary & Conclusions

A single parameter can be used as a first-order measure of a tire's wet traction performance. This is the fractional groove volume, represented by ϕ, and is the ratio of groove volume to total tread volume. Total tread volume is calculated on the basis of the developed (in-contact) tread width and a reference depth dimension, normal to the tread surface.

Both the locked-wheel or slide braking traction coefficient, μ_s, and the cornering coefficient, μ_c, exhibit an exponential dependence on ϕ, such that μ_s or μ_c approaches an upper or maximum limit as ϕ is increased. The exponential curve so established is representative of fixed external conditions ie. pavement texture, test speed, water depth and other non-pattern tire features. This exponential behavior

is observed in the 60-100 KPH (40-60 MPH) test speed range for the conditions used in the testing of this program. At low speeds, 30-50 KPH (20-30 MPH), especially under high texture - thin water film conditions, there is very little dependence of μ on ϕ.

This behavior is explained on the basis of the mode of water lubrication. At low speeds the lubrication mode is mainly boundary layer and traction performance is primarily independent of ϕ apart from some minor influence in the low ϕ range (<0.10). At the higher speeds especially under low pavement texture - larger water depth conditions, the lubrication mode is mainly hydrodynamic and the exponential nature of the μ vs ϕ relationship is observed.

Some geometric features of tread patterns are not entirely accounted for by ϕ; these are the zig-zag or pitch and throw of circumferential grooves and the void contributed by transverse grooves. Statistical analysis shows that for the tires of this program, ϕ accounts for 71% of the total μ_s variation and the other above geometric features and test error account for the remaining 29%. It is postulated that the adverse effects of groove pitch-throw on μ_s are due to an increased hydraulic resistance of front-to-rear water flow in the contact patch. Increased pitch-throw is not detrimental to μ_c (wet cornering traction) at high speeds 100 KPH (60 MPH). This is an important traction mode. Thus it is not possible to generalize about the fine geometric details of tread patterns.

Pavement void or macrotexture acts in an analogous manner to tread pattern void. The locked-wheel wet braking traction coefficient shows an exponential dependence on texture number and approaches a limiting value as textured is increased at fixed external conditions. In this experiment pavement microtexture was essentially equal for the various pavements used.

The concept of operational severity is discussed. This is a function proportional to speed and water depth and inversely proportional to pavement texture, (micro and macro), tread void volume and other tire parameters. Tires should be evaluated for wet traction performance at high operational severities. This provides for maximum discrimination in traction potential. The exponential or asymptotic behavior of μ vs ϕ curves and the countervailing effects that continued increase in ϕ has on tire wear resistance and dry pavement handling characteristics, requires an optimum balance approach to tire tread pattern design.

The author extends thanks to the B.F.Goodrich Co. for permission to publish this paper.

APPENDIX I

Terminology and Nomenclature

α = tire slip angle, deg or rad

F_x = longitudinal traction force, KN, lbf.

F_y = lateral traction force, KN, lbf.

F_z = normal force (tire load), KN, lbf.

μ_s = (wet slide braking coefficient)

$\mu_s = (F_x/F_z)_s$; s = slide or locked wheel mode

μ_c = (wet cornering coefficient)

$\mu_c = \left(\frac{\text{Cos } \alpha \, F_y}{F_z} \right)_c$; c = cornering traction mode

μ_p = (wet peak braking coefficient)

$\mu_p = (F_x/F_z)_p$; p = peak or transient value prior to wheel lock-up

D_W = water depth, mm or inch, either $D_{W(aa)}$ or $D_{W(cla)}$ see Appendix III

V = vehicle velocity, KPH or MPH

Tx_F = fine scale or microtexture of pavement, in range of 0.1 mm or less

Tx_L = large scale or macrotexture of pavement, visible aggregate particles and intervening voids in the range of one mm or greater

υ_{TR} = general term for tread pattern void

P_T = tire parameter

W_G = circumferential groove width, mm

W_R = rib width, mm

W_{TG} = width of transverse groove, mm

N_G = number of grooves in tread pattern

N_R = number of ribs in tread pattern

h_o = arbitrary reference depth of tread, mm

h_G = measured (average) groove depth, mm

d_{TW} = developed or loaded contact tread width, mm

ϕ = ratio of groove volume to total tread volume (referenced to a 10 mm tread depth and using d_{TW})

ψ = ratio of unused to total potential traction at any given set of external conditions

(ψ_s = traction measured by μ_s)

(ψ_c = traction measured by μ_c)

APPENDIX II

Test Procedures Used for Wet Traction Measurements

Test Vehicles. The braking traction tests were conducted with a special test trailer that conforms to the specifications set forth in ASTM E-274. Braking force of F_x and normal force or tire load F_z were measured with a bi-axial force cell and their ratio (μ_s) was calculated in real time and recorded.

The cornering force measurements were conducted with a two-wheel cornering force trailer that has been previously described (16). Cornering force was measured for a one second period at a slip angle α of 12°. Division of the cornering force, F_y cos α by the normal force F_z yields the cornering coefficient, μ_c.

Test Sequences and Test Surfaces. Testing with both trailers was conducted at target speeds of 32,48,64,81,96 KPH (20,30,40,50 and 60 MPH). The measured traction coefficients were plotted vs the measured speed and from a linear regression analysis the constants of the linear equation listed below were evaluated.

$$\mu = b_0 + b_1 V \qquad (1)$$

where:

μ = either μ_s or μ_c

V = speed, KPH or MPH

b_0 = intercept or μ at V = o

b_1 = slope = $d\mu/dv$

Several runs at each speed were used. Any quoted traction coefficient is obtained as an interpolated value at a definite speed using the linear regression equations. Tire load (normal force) was in the range of 85 - 100% of T & R rated load at 166 KPa (24 psi) and all tests were conducted 190 KPa (28 psi) tire pressure. Figure 7 shows the good linearity of some typical μ_s vs V plots and the monotonic decrease of μ_s to essentially zero values at high speeds. Similar plots are obtained for μ_c.

Figure 7. Typical Curves of μ_s vs Speed on Test Surfaces A and J. (See Appendix II).

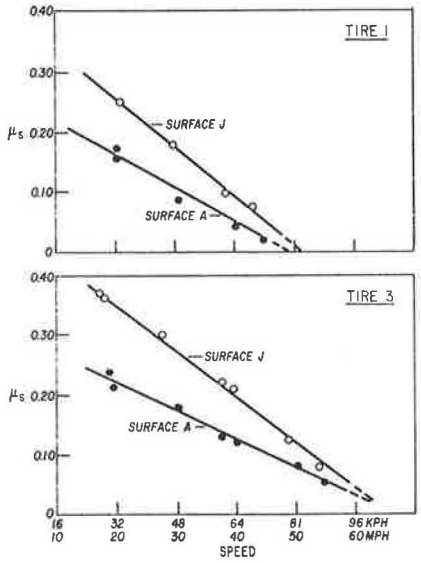

Three: low traction" test surfaces were used for the main testing program. These are located at Automotive Proving Grounds, Pecos, Texas and are designated as A,G. and J. Pertinent details are:

Surface A - A Portland cement concrete surface that was longitudinally brushed prior to set up. After complete hardening these longitudional ridges were ground with a terazzo grinding machine until the wet traction level was considerably lowered.

Surface G - This is coarse aggregate - Bituminous pavement plus blow sand.

Surface J - This was identical to the non-ground but brushed base surface used for Surface A. Rather than grinding the brushed surface was sand-blasted to moderately reduce the traction level.

The macrotexture of these three surfaces is in the order of A,J,G. See Figure 8 for photographs of these surfaces.

Water Application - Wind Protection. All wet traction tests are conducted with external water application via oscillating sprinklers located every 6 meters (20 ft.) along the edge of the skid surface. The oscillation rate was 2 per minute at a line pressure of 207 KPa (30 psi). A one percent cross-slope allowed for lateral water drainage. Water application was on the wind-ward side. It has been shown that the wet cornering coefficient, shows a negative μ_c vs log D_W dependence at high speeds and at fixed pavement texture (17). Surface water depths, often vary by a ratio of 3 to 1 or more due to wind velocity changes (magnitude and direction). Such changes can have a substantial influence on high speed wet traction measurements, and must be reduced as much as possible in any serious wet traction testing.

To reduce the influence of the lateral wind velocity component on the static water depth, wind barriers were used. These consisted of an A-frame construction using 1.2 m (4 ft.) high snow fence with vertical slats 25mm wide, with a 40mm opening between slats. These barriers were located along the edge of the test surface at the marked test zones. All tests were conducted at these specific zones. The use of these wind barriers is quite efficient and the influence of wind on water depth is reduced to one-tenth of its value under open or non-protected conditions.

Figure 8. Photographs of Test Surfaces A,G, and J. (See Appendix II).

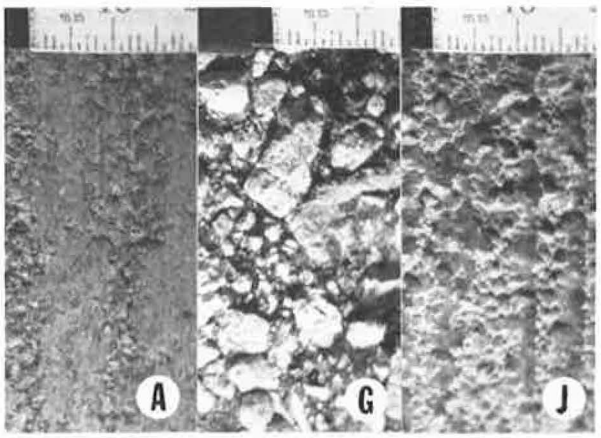

APPENDIX III

Measuring Water Depths on Tire Traction Skid Surfaces

Two methods have been used to measure the depth of water films on test surfaces. These films are quasi-static, a low velocity water flow takes place during testing due to pavement slope and a small component due to wind induced flow.

Figure 9. Illustrations Defining $D_W(aa)$ and $D_W(cla)$.

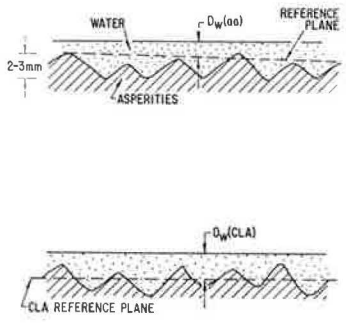

Above Asperity Depth, $D_W(aa)$. This depth is indicated in the upper sketch of Figure 9, it is the height above the local average asperity height in a small circular test zone. It is measured with a meter previously described (16) (17). In this meter

a series of electrical contact pins are arranged in a stair-step fashion with 0.25mm (0.01 inch) increments referenced to a base plane which is coincident with the top-of-the asperity plane. To monitor test surface water depths, 12-18 depth measurements are made at precisely located and uniformly distributed measurements sites on the skid surface. This depthmeter is satisfactory for any reasonable depth (0.3mm) on relatively smooth surfaces and for moderate to large depths (1.3 mm) on highly textured surfaces.

Center-line Average Depth, D_W(cla). This depth as indicated in the lower sketch of Figure 9, is a depth that might be grossly termed a total water depth. It is measured by placing on the wet skid surface, a 150mm (6 inch) diameter cylinder with a specially designed rubber sealing ring around its lower circular periphery. The water trapped in this circular zone is quickly absorbed with an absorbent pad of known weight and the amount of water in the circular zone is determined by weighing the pad. The (weight) volume is translated to a depth based on calculations of the effective inside circular area and on the basis of a standard smooth "substrate" surface. For on-the-pavement water depths with their upper surface above the Cla plane, there is no conceptual problem. The Cla effectively averages out the hills and valleys of the aggregate asperities and this Cla value acts as a lower reference plane for water depth. For highly textured pavements with a very minimum of water, negative depths are possible. The water application rates and measured depths of this program were sufficiently large to preclude this occurence.

Both of these water depth "meters" are constructed so that measurements can be made under normal water application or "test" conditions; ie. with oscillating sprinklers on skid pads, or during an actual rainfall period. Special precautions are taken to prevent any spurious splash effects during measurement.

Water depths on these surfaces during the testing were as follows:

Surface	D_W(aa)		D_W(Cla)	
	mm.	in.	mm.	in.
A	0.53	(0.021)	1.1	(0.042)
J	0.89	(0.035)	1.4	(0.057)
G	0.31	(0.012)	1.8	(0.069)

These represent averages of 12-18 locations on each surface. For daily depth monitoring, exact locations are marked on the pavement. This allows a depth meter positioning accuracy of $\pm$ 12 mm (0.5 inch).

The precision of depth measurement at any one location is 9.5% expressed as a coefficient of variation. The variation of depth along the test surface has a coefficient of variation of 28% and thus a sufficient number of locations (12-18) must be included for an accurate depth assessment. The distribution of depths has been found to be normal in a statistical sense.

APPENDIX IV

Characterizing Groove "Zig-Zag" Geometry

The "zig-zag" geometry of tread grooves may be characterized by the use of the terms pitch and throw. These are defined in part A of Figure 15. Throw is the maximum lateral displacement from a circumferential reference line for each groove and pitch is the "one-wave length" spacing around the tire circumference. To reduce noise tonality, groove pitch is varied around the circumference in commercial tread designs.

Increasing the degree of pitch and throw increases the in-the-groove path length between any two points along the circumference. This increased path length can be calculated by replacing the actual groove with a line as depicted in Part B of Figure 15. It can be shown from geometry that the length of the line segment a b compared to a'b' is given by the ratio RCL.

$$RCL = \frac{\sqrt{T^2 + \left(\frac{P}{2}\right)^2}}{\left(\frac{P}{2}\right)} \qquad (1)$$

where RCL is defined as the Relative Channel Length.

Figure 15. Illustrations Defining Pitch (P) and Throw (T) and Relative Channel Length or RCL. (See Appendix IV).

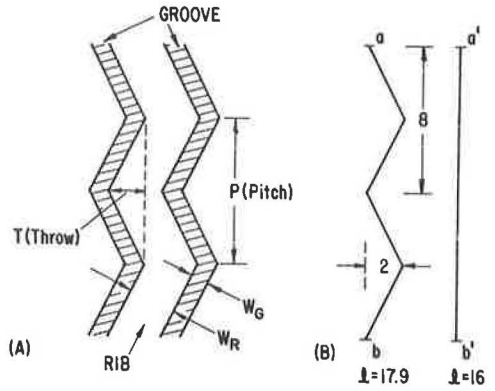

For the lines illustrated, a'b' = 16 units, ab = 17.89 $\cong$ 17.9 units as calculated by (1). Thus RCL = 1.118 for line a'b' compared to line ab. RCL values will vary between unity and an upper value of approximately 1.30 for most tread patterns.

APPENDIX V

Pavement Drainage Measurement for Macrotexture Characterization

D.F. Moore (5), (15) has published numerous papers on the measurement of pavement texture. For this purpose a water drainage or outflow meter was devised, which consists of a circular cylinder with a square cross-section circular rubber ring attached to the bottom periphery. This is placed vertically on a road pavement, loaded to a predetermined value and the time of efflux of a known quantity of water is measured. From a knowledge of the dimensions of the cylinder and the rubber ring, a term defined as the mean hydraulic radius (MHR), may be calculated. This is the ratio of the periphery of the flow channels under the ring to their cross-sectional area and is a measure of the macrotexture of a pavement.

The MHR is given by

$$MHR = C_1 \sqrt[4]{\frac{\gamma}{t\, n^{\frac{1}{2}}}} \qquad (1)$$

where γ = viscosity of water

t = outflow time, sec.

n = number of asperities per 6.5 cm^2 ($inch^2$)

C_1 = an instrument constant

The outflow meter used for the drainage measurements of this report was not calibrated. The results therefore are equivalent to MHR/C_1. Rather than report this, a pavement texture number was calculated for each test surface.

Thus rearranging (1)

$$N_{PT} = \frac{MHR}{C_1\, \gamma^{\frac{1}{4}}} = \left(\frac{1}{t\, n^{\frac{1}{2}}}\right)^{\frac{1}{4}} \qquad (2)$$

where N_{PT} = pavement texture number, a term directly proportional to MHR.

It has been found that N_{PT} follows a statistically normal distribution with a typical coefficient of variation of 9%. It is important to note that outflow times per se are not reliable indicators of pavement texture due to the varying texture of the pavement. The following range of t values illustrates this.

Surface	N_{PT}	Range of t (Max - Min)
F*	3.8	268 - 203 sec.
A	9.1	164 - 17.4
J	11.7	40.9 - 6.7
G	19.7	8.6 - 3.9

*(smooth) polished concrete.

The reported N_{PT} values are averages of from 16 to 30 measurements depending on the surface, but all measurements located in the traction test zones.

References

(1) D.F. Moore, "The Friction and Lubrication of Elastomers" Pergammon Press LTD. 1972.

(2) D. Downson, Chapter in "Boundary Lubrication An Apprasal of World Literature" Ed. by K. Klung, E. Klaus, R. Fein, ASME Spec. Publication N.Y. (1969).

(3) D. Dowson, G.R. Higginson "Elasto-Hydrodynamic Lubrication" Pergammon Press LTD. 1966.

(4) V.E. Gough, Discussion of paper by D. Tabor, Rev. Gen. Caoutchouc 36. (10) 1409 (1959).

(5) D.F. Moore, Wear 8, 245 (1965).

(6) G. Lees, A.R. Williams, Jour. IRI 8, 114 (1974). Also ASTM E-451-72.

(7) B.E. Sabey, C.G. Giles, G. Grimes. Proc. Auto Div. Inst. Mech. Engineers 19, (1954-55).

(8) W.E. Meyter, (Pennsylvania State Univ.) SAE Paper 710572 (June 7-11), 1971.

(9) D.L. Ivey, R.M. Gallaway (Tex. Trans. Inst.) Highway Research Board H471 13-26, (1973).

(10) D.F. Dunlap, P.S. Fancher, Jr., R.E. Scott, C.C. MacAdam and L. Segel - "Passenger Car Skidding as Influenced by Roadway Design, Tire Tread Depth and Pavement Conditions", Hit Lab Reports 5, Dec. (1974). Highway Safety Research Institute, Ann Arbor, Michigan.

(11) H. Williams, Tire Science & Technology 3, 267 (1975).

(12) A. Schallmach, Skid Resistance & Directional Control - Chapter 6 in "Mechanics of Pneumatic Tires", Ed. S.K. Clark National Bur. of Stds. Monograph 122 (1971).

(13) M.H. Walters, Paper #3, "Symposium on Friction and Wear in Tires" Proc. of D. Mat (Av) Conference, Oct. 2, 1968, London, England.

(14) K.B. Wallace, D.H. Trollop Wear 13, 109 (1969).

(15) D.F. Moore, J. of Royal Aeronautical Soc. 69, 337 (1965).

(16) A.G. Veith, R. Chem. & Technology 44, 962 (1971).

(17) A.G. Veith & M.G. Pottinger, Paper #1, Session 1 (pp 5-24) Symposium on "Physics of Tire Traction" published Plenum Press N.Y., 1974.

(18) B.A. Sabey, J. of British Granite and Whinstone Federation 5 (2), 1 (1965).

(19) L. Holla, W.O. Yandell, J. of Australian Road Res Board 5, 76 (1973).

(20) R.A. Moyer, First Int'l Skid Prevention Conference Part II 411 (1959).

(21) J.G. Rose, B.M. Galloway, K.D. Hankins, Highway Res. Board 341, 33 (1970).

(22) B.J. Allbert, J.C. Walker, R. Chem. & Technology 41, 753 (1968), also Proc. Inst. Mech. Engineers (Auto Div.), 180, 2 A 105 (1965-66).

(23) A.H. Neill, NBS Technical Note 566 (Feb., 1971) and Automotive Eng. 79, 33 (1971).

(24) G. Maycock, R. Chem. & Technology 41, 780 (1968).

(25) J.D. Kelly, Jr., SAE Paper 680138, Jan 8, 1968.

(26) S.C. Britton, W.B. Ledbetter, B.M. Gallaway, Jour. Testing and Evaluation (ASTM) 2, 73 (1974).

(27) D.F. Moore, Highway Research Record 131, 181 (1966).

(28) R.N. Doty, Research Report CA-DOT-TL-3126-10-74-24 presented at ASTM Surface Texture Symposium, June 27, 1974, Washington, DC.

(29) A.G. Veith, "Tire Wear – Some Knowns and Unknowns" Paper presented to Technical Meeting of Akron Rubber Group on January 25, 1974.